



Introduction of novel characteristic time quantities to describe chemical reactors

Christian Weiland^{*}, Mustafa Salli, Jürgen Fitschen, Marko Hoffmann, Michael Schlüter

Institute of Multiphase Flows, Hamburg University of Technology, Eißendorfer Straße 38, Hamburg 21073, Germany

ARTICLE INFO

Keywords:

Mean distribution time
Mean dead time
Local residence time Distribution
Mixing efficiency
Reactor characterization
Computational fluid dynamics

ABSTRACT

The Mean Residence Time is a quantity which is used very often to characterise chemical reactors. This quantity can be calculated using the Residence Time Distribution of a specific, continuous reactor and assuming closed-closed boundary conditions. Many reactors in the industry though, are discontinuous ones and the direct application of these methods is in general not possible. This work presents a new distribution, the Local Residence Time Distribution, which observes each position in a specific reactor. Furthermore, two new, local quantities, the Mean Distribution Time and the Mean Dead Time, are introduced, which can be applied as characteristic times to evaluate the internal behaviour of chemical reactors used for discontinuous processes such as fermentations.

1. Introduction

In many applications in the chemical and biochemical industry, the mixing efficiency has a deep impact on the whole process [1]. As dominant characteristic, the Residence Time Distribution (RTD) and the Mean Residence Time (MRT) [2] are established as reliable tools to judge the efficiency of continuous reactors [3–5]. Nevertheless, both quantities have significant disadvantages, since they only evaluate global effects [6] and are restricted to continuous processes with an inlet and an outlet. Further, the closed-closed boundary condition is often assumed, stating that a fluid element which has left the reactor will not enter it again and that no fluid element will leave the reactor through the inlet [7]. For discontinuous processes, like those carried out in stirred tank reactors (STR), these mechanisms are not applicable directly due to the possibility of missing inlets or outlets and thus the missing applicability of the closed-closed boundary condition. In the past, Ghirelli and Leckner have examined the local residence time for a system with an inlet and an outlet [8]. Further, Xiao et al. have observed the local residence time of particles in a fluidised bed with recirculation [9]. In this work, two novel quantities, the *Mean Distribution Time* (MDiT) and the *Mean Dead Time* (MDeT), are presented as an extension of the already existing tools to characterise also discontinuous reactors with such time characteristics. Both quantities focus on the local instead of global time characteristics of such vessels and will be evaluated in a stirred tank reactor (STR) by means of numerical simulations utilising the Lattice

Boltzmann Method (LBM) using the programme M-Star CFD (M-Star Simulations, LCC.).

2. Material and methods

The definition of the MDiT and the MDeT will be presented in chapter 2.1. These quantities can be applied on continuous systems and will be estimated for an STR. The geometry of the STR will be presented in chapter 2.2. The final chapter 2.3 will explain how the estimation of the MDiT and the MDeT will be conducted.

2.1. Mean distribution time and mean dead time

The RTD $F(t)$ can be calculated for a continuous reactor by measuring the concentration of a specific tracer $c_{\text{out}}(t)$ at the reactor's outlet after the addition of the tracer as step function $c_{\text{in}}(t) = c_{\infty} \cdot \sigma(t)$ at the inlet, where [2]

$$\sigma(t) := \begin{cases} 0, & 0 > t \\ 1, & 0 \leq t. \end{cases} \quad (1)$$

The RTD is now achievable via

$$F(t) = \frac{c_{\text{out}}(t)}{c_{\infty}}. \quad (2)$$

Since the observed vessel is an STR with no outlet, a new definition is

^{*} Corresponding author.

E-mail address: christian.weiland@tuhh.de (C. Weiland).

<https://doi.org/10.1016/j.cej.2023.100534>

Received 28 April 2023; Received in revised form 21 June 2023; Accepted 13 July 2023

Available online 14 July 2023

2666-8211/© 2023 The Author(s). Published by Elsevier B.V. This is an open access article under the CC BY license (<http://creativecommons.org/licenses/by/4.0/>).

Arabic symbols		Greek symbols	
\dot{c}	Derivative of the concentration with respect to time	α	Factor to account for the optical depth
\hat{c}	Non-negative derivative of the concentration with respect to time	$\delta(\cdot)$	Dirac impulse
$\mathcal{T}_{\mathcal{H}}$	Mean Dead Time	η	Dynamic viscosity
$\mathcal{T}_{\mathcal{M}}$	Mean Distribution Time	Ω	Geometric space
$\mathcal{T}_{\mathcal{R}}$	Mean Residence Time	ρ	Density
\tilde{F}	Local Residence Time Distribution	$\sigma(\cdot)$	Step function
\mathbf{x}	Position	θ	Angle
c	Concentration	ϑ	Temperature
c_{∞}	Initial concentration	Abbreviations	
C_S	Smagorinsky constant	LBM	Lattice Boltzmann Method
Co	Courant-number	LES	Large Eddy Simulation
D_{ij}	Diffusion coefficient of species i in phase j	LRTD	Local Residence Time Distribution
F	Residence Time Distribution	MDeT	Mean Dead Time
n	Stirrer frequency	MDiT	Mean Distribution Time
p	Indicator function	MRT	Mean Residence Time
t	Time	RTD	Residence Time Distribution
V	Volume	STR	Stirred Tank Reactor

presented to account for the necessarily occurring violation of the closed-closed boundary condition, which is always assumed to determine the RTD and the MRT for continuous processes. Each point $\mathbf{x} := (x \ y \ z)^T \in \Omega$ of the whole domain $\Omega \subset \mathbb{R}^3$ is observed. Further, as input concentration a Dirac-impulse $c_{\text{in}}(t) = c_{\infty} \cdot \delta(\mathbf{x} - \mathbf{x}_0, t - t_0)$ is chosen, where $\mathbf{x}_0 \in \Omega$ is the feed position and t_0 the point in time at which the tracer is added. For each position \mathbf{x} , the Local RTD (LRTD)

$$\tilde{F}(\mathbf{x}, t) := \frac{\int_0^t \dot{c}(\mathbf{x}, \tau) d\tau}{\int_0^{t_{\infty}} |\dot{c}(\mathbf{x}, \tau)| d\tau} \quad (3)$$

can be defined, where t_{∞} is the latest, observed time and the dot relates to the derivative with respect to time. With this definition, the monotonically increasing behaviour and the limitation $0 \leq \tilde{F}(\mathbf{x}, t) \leq 1$ is guaranteed.

In analogy to the well-known definition of the MRT [10]

$$\mathcal{T}_{\mathcal{R}} = \int_0^{t_{\infty}} \tau \cdot \frac{dF(\tau)}{d\tau} d\tau \equiv \frac{1}{c_{\infty}} \int_0^{t_{\infty}} \tau \cdot \dot{c}_{\text{out}}(\tau) d\tau, \quad (4)$$

the MDiT

$$\mathcal{T}_{\mathcal{M}}(\mathbf{x}) := \frac{\int_0^{t_{\infty}} \tau |\dot{c}(\mathbf{x}, \tau)| d\tau}{\int_0^{t_{\infty}} |\dot{c}(\mathbf{x}, \tau)| d\tau} \quad (5)$$

and the MDeT

$$\mathcal{T}_{\mathcal{H}}(\mathbf{x}) := \frac{\int_0^{t_{\infty}} \tau \hat{c}(\mathbf{x}, \tau) d\tau}{\int_0^{t_{\infty}} \hat{c}(\mathbf{x}, \tau) d\tau} \quad (6)$$

are proposed as new quantities to characterise the mixing efficiency in discontinuous reactors with open-open boundary conditions for each position. Hereby is

$$\hat{c}(\mathbf{x}, t) := \begin{cases} \dot{c}(\mathbf{x}, t), & \dot{c}(\mathbf{x}, t) > 0 \\ 0, & \dot{c}(\mathbf{x}, t) \leq 0. \end{cases} \quad (7)$$

The MDiT is the time at which the concentration at the position \mathbf{x} experiences its most significant change. The MDeT is the time where the concentration at the position \mathbf{x} experiences a significant rise. For the MDiT and the MDeT $\mathcal{T}_{\mathcal{M}}(\mathbf{x}) \geq \mathcal{T}_{\mathcal{H}}(\mathbf{x})$, $\forall \mathbf{x} \in \Omega$ holds.

2.2. Stirred tank reactor setup

The numerical model of the STR has previously been introduced and experimentally validated by Kuschel et al., Hofmann et al. and Fitschen [11–13]. It has a working volume of $V_{\text{STR}} = 2.8 \text{ L}$. The reactor has a korbogen head bottom, three baffles with an angular offset of $\theta = 2\pi/3$ and two Rushton turbines. The reactor does not have an outlet. The relevant dimensions can be taken from Figure 1. The numerical properties of the fluid are those of water at $\vartheta = 20^\circ \text{C}$ ($\rho_F = 998.2 \text{ kg m}^{-3}$, $\eta = 1.0016 \text{ mPa s}$). The numerical reactor model matches a real reactor made of glass, at which optical measurements are conducted.

2.3. Procedure

The flow in the STR is simulated utilising the LBM using the programme M-Star CFD 3.6.13. Since the simulation is not the core of this work, only the relevant settings are presented briefly. A detailed description of the LBM in the course of this work was presented by Hofmann et al. [12]. A complete in depth derivation of the whole method can be found in the books by Krüger et al. [14] or Succi [15]. An equidistant grid with 300 lattice point across the vessel's diameter is chosen. This yields a distance between lattice points of $\Delta x_L = 0.42 \text{ mm}$. A Courant number of $Co = 0.05$ is used to guarantee stability. To account for turbulent effects, the simulations are conducted as Large Eddy Simulation (LES). As subgrid-scale model the Smagorinsky-Lilly model with a Smagorinsky constant of $C_S = 0.1$ is chosen [16]. A stirrer frequency of $n = 252 \text{ rpm}$ is set. After $t_{\text{stat}} = 20 \text{ s}$ a quasi-stationary state is reached. At this time, the tracer is added as Dirac-impulse with a concentration of $c_{\infty} = 1 \text{ mol L}^{-1}$ at two positions directly below the interface at a height of $y = 0.228 \text{ m}$. The exact positions in the $x - z$ -plane can be taken from Fig. 2. The diffusion coefficient of the tracer in water is $D_{\text{T,H}_2\text{O}} = 9.31 \times 10^{-9} \text{ m}^2 \text{ s}^{-1}$. The concentration is saved on in total $m = 62$ equidistant output planes every second. The output planes are normal to the z -direction, the respective position in the z -direction is z_k , $k = 1, \dots, m$. They are depicted as red lines in Fig. 2. For the calculation of the MDiT and the MDeT on the output planes, the integrals in Eqs. (5) and (6) are approximated by the application of the trapezoidal rule [17]. For visualisation, the values of the MDiT and the MDeT on the output planes are summed up in the z -normal direction to be projected onto the $z \equiv 0$ -plane

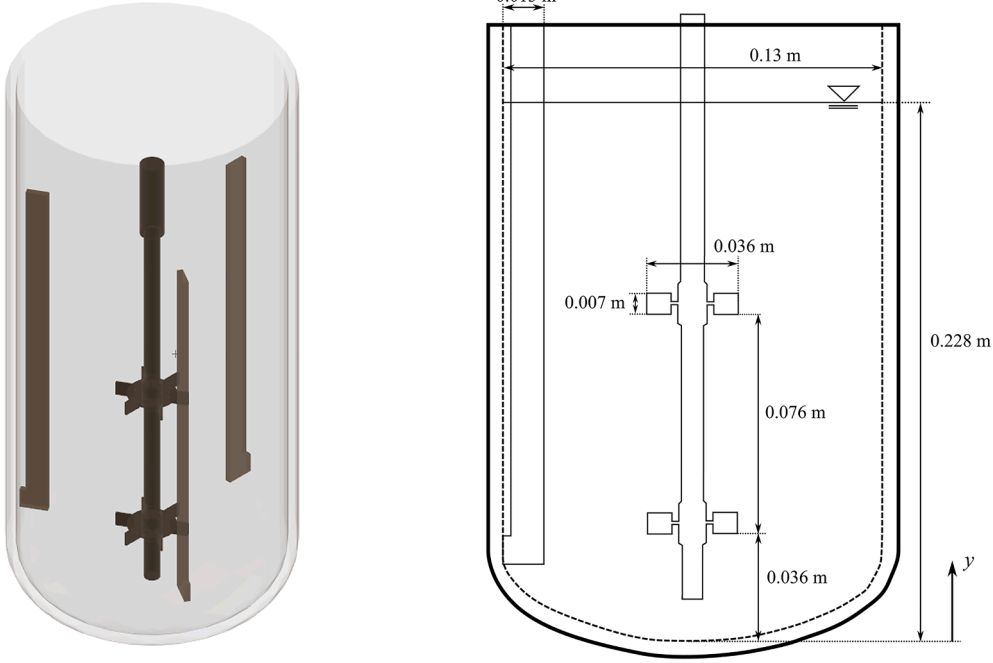


Fig. 1. Geometric setup and dimensions of the STR.

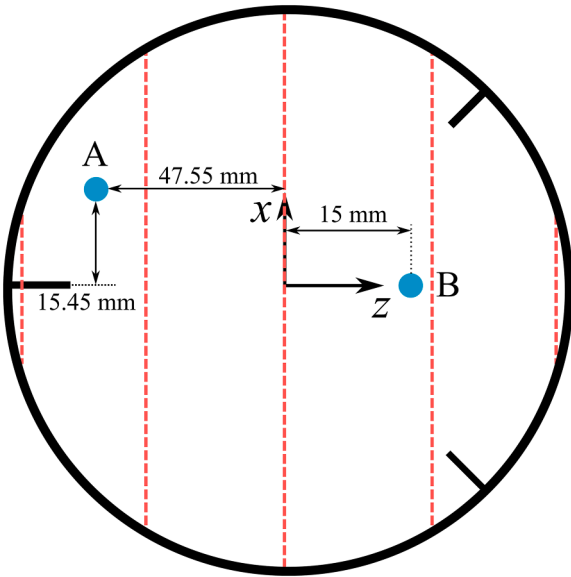


Fig. 2. Positions of the two feed positions A and B (turquoise) and a schematic depiction of the output planes (red).

$$\mathcal{T}_{\mathcal{A},\text{proj}}(x, y) = \alpha(x, y) \cdot \sum_{k=1}^m \mathcal{T}_{\mathcal{A}}(x, y, z_k) \quad (8)$$

$$\mathcal{T}_{\mathcal{B},\text{proj}}(x, y) = \alpha(x, y) \cdot \sum_{k=1}^m \mathcal{T}_{\mathcal{B}}(x, y, z_k). \quad (9)$$

To take into account the optical depth and to make the results comparable with experimental data achieved by optical measurements, the projected quantities are multiplied with a factor $\alpha(x, y)$ with

$$\frac{1}{\alpha(x, y)} = \sum_{k=1}^m p(x, y, z_k), \quad (10)$$

where

$$p(x, y, z_k) = \begin{cases} 1, & (x \ y \ z_k)^T \in \Omega \\ 0, & (x \ y \ z_k)^T \notin \Omega \end{cases} \quad (11)$$

is an indicator whether the observed position is part of the relevant domain Ω or not. This information is delivered directly by M-Star CFD. Hence, the factor $\alpha(x, y)$ takes into account the optical depth and the achieved results can be compared with experimental data from optical measurements, e.g. decolourisation experiments with a neutralisation reaction. Such experiments have been conducted by Fitschen et al. [6].

3. Results and discussion

The results concerning the MDiT and the MDeT for the relevant STR using a stirrer frequency of $n = 252$ rpm are shown in Fig. 3. First of all, it can be seen that both time quantities are qualitatively similar, but the MDiT at each position is slightly higher than the MDeT at the same position. The highest values can be found at the bottom of the vessel, which is due to the feed position at the surface. Both time quantities match each other at the lower regions. In the upper part of the STR, the MDiT and the MDeT are lower and varying more strongly. The reason is also for this case the feed position. Directly after the feed addition, dynamic concentration changes are to be expected in the upper regions. Further investigation yields the identification of possible occurring compartments, dividing the reactor in separated regions of various mixing dynamics. The area of the steepest gradient in the y -direction can be found between the two stirrers, indicating a compartmentalisation at this point. This finding matches the experimental results from Fitschen [13] who proposed the observation of the propagation time and the numerical results from Weiland et al. [18] who identified coherent sets with Lagrangian methods. The comparison of the values of the MDiT and the MDeT yields a high sensitivity to the feed positions. The values for both quantities differ strongly in the region near the respective feed position. The influence in the lower regions of the STR is not as significant as in the upper regions, but also there differences of up to 10 % can be found. The reason for this could be the fact that the position B is directly between two baffles. Weiland et al. [18] have shown that at this

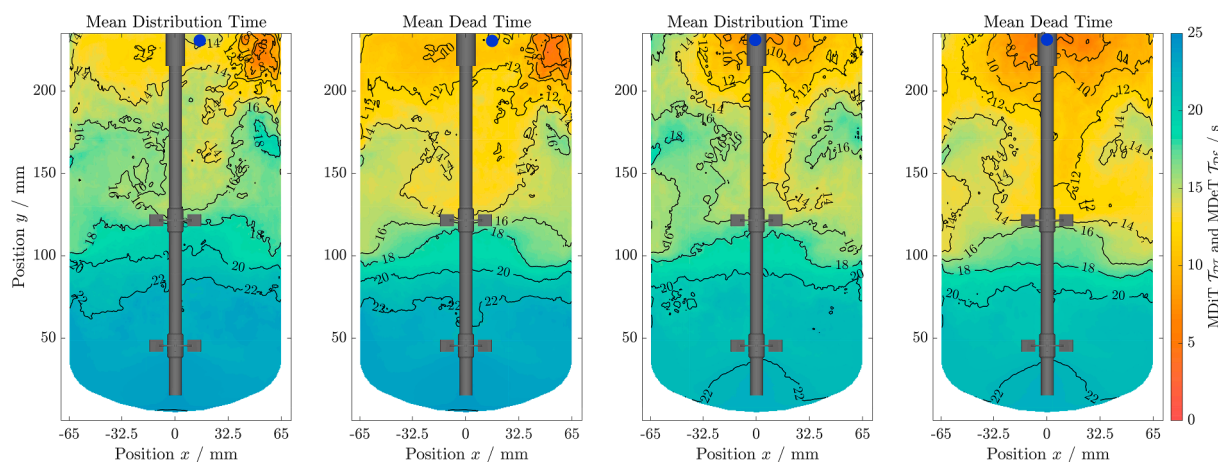


Fig. 3. Projected MDiT and MDDeT for feed positions A and B (blue dots) and a stirrer frequency of $n = 252$ rpm.

position a compartment exists. With this dominant influence on the flow, the transport of species added here into other regions of the vessel is slowed strongly. The influence of another compartment can be seen in the results for feed position A. The lowest MDiT and MDDeT are directly at the position of this other compartment, also covering the findings of Weiland et al. [18].

These new quantities are now compared with commonly known quantities such as the mixing time t_{95} as described by Nienow [19], cf. Fig. 4. Obviously, both characteristic time quantities show a completely different image of the mixing efficiency. This is due to the fact that the local mixing time is the time from which on no larger deviations than 5% of the mean value can be observed, while the MDiT and the MDDeT mirror the time at which the most significant change or rise, respectively, is to be expected. Compared to results from optical measurements via conducting a neutralisation reaction carried out by Fitschen et al. [6], the benefits of the MDiT and the MDDeT become obvious, cf. Fig. 5.

Qualitatively, those new, simulatively retrieved quantities match the experimentally retrieved mixing time distribution well. The zones of high and poor mixing efficiency match for both cases qualitatively. The deviation of the simulated local mixing time, shown in Fig. 4 on the other hand can be explained with the experimental procedure. Those results are achieved by measuring the grey value during a neutralisation reaction. Indicators like bromothymol blue only have a specific range in which they are coloured. Due to that, concentration overshoots are not

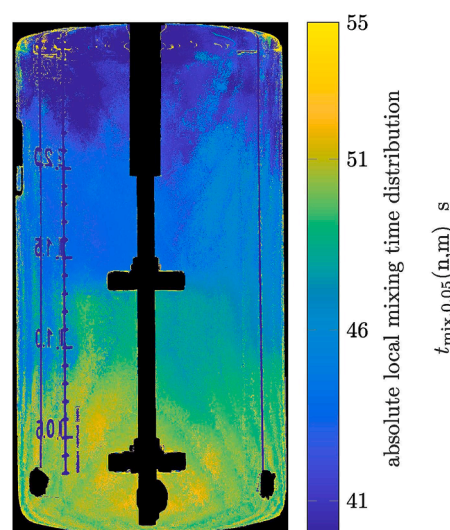


Fig. 5. Absolute local mixing time distribution by means of bromothymol blue and an acid to base ratio of 1:1 at $P/V = 7.3 \text{ W m}^{-3}$, taken from [6], please pay attention to the changed colouring

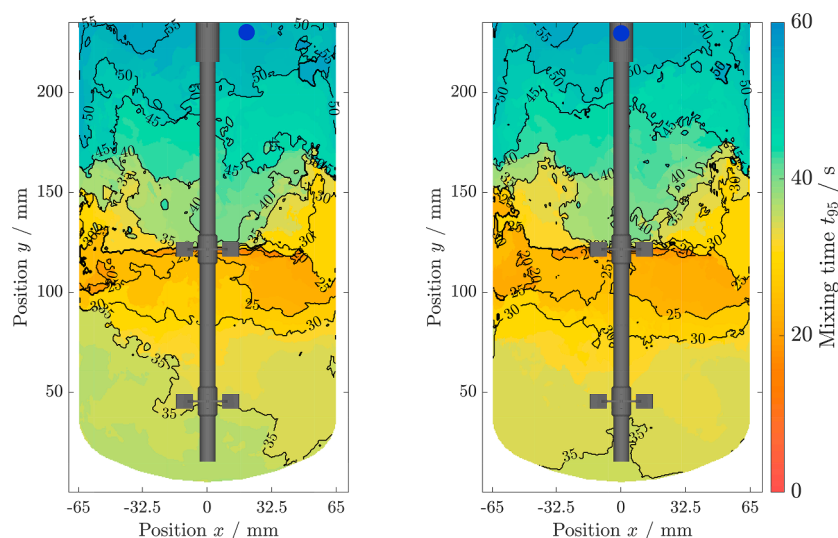


Fig. 4. Projected local mixing time t_{95} for feed positions A and B (blue dots) and a stirrer frequency of $n = 252$ rpm.

measurable with this method. Further, this kind of reaction is often rather fast, resulting in a rapid decolourisation near the feed position.

4. Conclusions

In this work, two new quantities, namely the Mean Distribution Time and the Mean Dead Time, are presented. The definitions are based on the already existing and well-known Mean Residence Time and the connection to the Residence Time Distribution for a continuous system. Since the processes inside of an STR are discontinuous, these two novel quantities are defined to yield knowledge not only about a global but about a local characteristic concerning mixing processes. For this purpose, the Local Residence Time Distribution was proposed for such discontinuous processes.

The MDiT and the MDeT are evaluated for an STR with a volume of 2.8 L after the addition of a tracer as Dirac-impulse at two different feed positions. The values are projected on a plane for visualisation and comparison with experimental results. The achieved results show the time of the most significant change and the most significant rise of the tracer concentration, respectively, allowing to make statements on the mixing performance of the observed STR by using these specific feed positions. Both quantities deviate strongly from the classical mixing time t_{95} , which mirrors the time from which on the content of a vessel is homogenised. With this knowledge, processes such as fermentations can be optimised by e.g. adjusting the feed position to reach the desired MDiT. Further, those time quantities can be used to more efficiently control a process, due to the known dead time between measures to force it into the desired direction and the response at each position.

Altogether, the MDiT and the MDeT form two quantities, which expand the already existing toolkit to characterise chemical reactors. They can be applied on discontinuous apparatuses and also when the closed-closed assumption is not suitable or the internal processes are of further relevance. With this, the MDiT and the MDeT can grant the respective operator more insight into their process and the opportunity to carry it out in a desired manner.

Data and code availability

Please contact the corresponding authors to obtain access to the data.

Declaration of Competing Interest

The authors declare that they have no known competing financial interests or personal relationships that could have appeared to influence the work reported in this paper.

Data availability

Data will be made available on request.

Acknowledgements

The authors thank Johannes Wutz from M-Star Simulations, LCC. for

the fruitful discussions.

Further, the authors thank Marc Maly for proofreading.

References

- [1] M. Zlokarnik, *Stirring: Theory and Practice*, Wiley-VCH, Weinheim ; New York, 2001.
- [2] P. Danckwerts, Continuous flow systems: distribution of residence times, *Chem. Eng. Sci.* 2 (1) (1953) 1–13, [https://doi.org/10.1016/0009-2509\(53\)80001-1](https://doi.org/10.1016/0009-2509(53)80001-1).
- [3] E.B. Nauman, Residence time theory, *Ind. Eng. Chem. Res.* 47 (10) (2008) 3752–3766, <https://doi.org/10.1021/ie071635a>.
- [4] A.E. Rodrigues, Residence time distribution (RTD) revisited, *Chem. Eng. Sci.* 230 (2021) 116188, <https://doi.org/10.1016/j.ces.2020.116188>.
- [5] B. Platzter, K. Steffani, S. Große, Möglichkeiten zur vorausberechnung von verweilzeitverteilungen: möglichkeiten zur vorausberechnung von verweilzeitverteilungen, *Chem. Ing. Tech.* 71 (8) (1999) 795–807, <https://doi.org/10.1002/cite.330710805>.
- [6] J. Fitschen, S. Hofmann, J. Wutz, A. Kameke, M. Hoffmann, T. Wucherpfennig, M. Schlüter, Novel evaluation method to determine the local mixing time distribution in stirred tank reactors, *Chem. Eng. Sci.* X 10 (2021) 100098, <https://doi.org/10.1016/j.cesx.2021.100098>.
- [7] F.F. Rivera, M.R. Cruz-Díaz, E.P. Rivero, I. González, Analysis and interpretation of residence time distribution experimental curves in FM01-LC reactor using axial dispersion and plug dispersion exchange models with closed-closed boundary conditions, *Electrochim. Acta* 56 (1) (2010) 361–371, <https://doi.org/10.1016/j.electacta.2010.08.069>.
- [8] F. Ghirelli, B. Leckner, Transport equation for the local residence time of a fluid, *Chem. Eng. Sci.* 59 (3) (2004) 513–523, <https://doi.org/10.1016/j.ces.2003.10.013>.
- [9] H. Xiao, Y. Zhang, J. Wang, Correlating measurement qualities of cross-correlation based solids velocimetry with solids convection-mixing competing mechanism in different gas fluidization regimes, *Chem. Eng. Sci.* 253 (2022) 117602, <https://doi.org/10.1016/j.ces.2022.117602>.
- [10] E. Müller-Erlwein, *Chemische Reaktionstechnik*, Springer Fachmedien Wiesbaden, Wiesbaden, 2015, <https://doi.org/10.1007/978-3-658-09396-9>.
- [11] M. Kuschel, J. Fitschen, M. Hoffmann, A. von Kameke, M. Schlüter, T. Wucherpfennig, Validation of novel lattice Boltzmann large eddy simulations (LB LES) for equipment characterization in biopharma, *Processes* 9 (6) (2021) 950, <https://doi.org/10.3390/pr9060950>.
- [12] S. Hofmann, C. Weiland, J. Fitschen, A. von Kameke, M. Hoffmann, M. Schlüter, Lagrangian sensors in a stirred tank reactor: comparing trajectories from 4D-particle tracking velocimetry and lattice-Boltzmann simulations, *Chem. Eng. J.* (2022) 137549, <https://doi.org/10.1016/j.cej.2022.137549>.
- [13] J. Fitschen, *Hydrodynamic Characterization of Heterogeneities in Aerated Stirred Tank Reactors: From an Eulerian to a Lagrangian Perspective*, 1. auflage, Cuvillier Verlag, Göttingen, 2022. Doctoral Thesis, Hamburg University of Technology, OCLC: 1348183249.
- [14] T. Krüger, H. Kusumaatmaja, A. Kuzmin, O. Shardt, G. Silva, E.M. Viggien, *The Lattice Boltzmann Method: Principles and Practice*, Springer Berlin Heidelberg, New York, NY, 2016.
- [15] S. Succi, *The Lattice Boltzmann Equation: For Fluid Dynamics and Beyond*, in: *Numerical Mathematics and Scientific Computation*, Clarendon Press, 2001. https://books.google.de/books?id=OC0Sj_xgnhAC.
- [16] J. Smagorinsky, General circulation experiments with the primitive equations: I. The basic experiment, *Mon. Weather Rev.* 91 (3) (1963) 99–164, [https://doi.org/10.1175/1520-0493\(1963\)091<0099:GCEWTP>2.3.CO;2](https://doi.org/10.1175/1520-0493(1963)091<0099:GCEWTP>2.3.CO;2).
- [17] P. Deuffhard, A. Hohmann, *Numerische Mathematik*, in: *De Gruyter Studium*, De Gruyter, Berlin, Boston, 2019.
- [18] C. Weiland, E. Steuwe, J. Fitschen, M. Hoffmann, M. Schlüter, K. Padberg-Gehle, A. von Kameke, Computational study of three-dimensional Lagrangian transport and mixing in a stirred tank reactor, *Chem. Eng. J. Adv.* 14 (2023) 100448, <https://doi.org/10.1016/j.cej.2023.100448>.
- [19] A. Nienow, On impeller circulation and mixing effectiveness in the turbulent flow regime, *Chem. Eng. Sci.* 52 (15) (1997) 2557–2565, [https://doi.org/10.1016/S0009-2509\(97\)00072-9](https://doi.org/10.1016/S0009-2509(97)00072-9).